

# Detection of Ionizing Radiation Using Graphene Field Effect Transistors

Michael Foxe\*, *Student Member, IEEE*, Gabriel Lopez\*, *Student Member, IEEE*, Isaac Childres, Romaneh Jalilian, Caleb Roecker, John Boguski, Igor Jovanovic<sup>#</sup>, and Yong P. Chen<sup>#</sup>, *Member, IEEE*

**Abstract**— We propose schemes of using graphene field effect transistors (GFET) to detect ionizing radiation. The detection is based on the high sensitivity of graphene to local change of electrical field that can result from the interaction of radiation with a semiconductor substrate in a GFET. We present preliminary modeling and experimental work to develop a prototype sensor, and discuss potential advantages compared to conventional detectors.

## I. INTRODUCTION

HIGH-PERFORMANCE sensors for penetrating ionizing radiation ( $\gamma$ -rays and neutrons) are important for many applications, for example, in nuclear security to facilitate detection of special nuclear materials (SNM) with high signal-to-noise ratios. A major challenge in the development of radiation sensors, particularly those for  $\gamma$ -rays, is achieving high energy resolution at room temperature. We are exploring the exceptional electronic properties of graphene (a single atomic layer of graphite) [1] to develop graphene-based devices with a potential to improve the performance of radiation sensors.

Here we present the operation schemes, and the preliminary results of our modeling and experimental work on graphene-

based radiation detectors (GRD). Our prototype device is a graphene field effect transistor (GFET) [2], consisting of graphene on a radiation-absorbing, electrically gated undoped semiconductor substrate (with a thin dielectric buffer layer in between). The technical approach is to utilize the dependence of the electrical conductivity of graphene on a local electric field, which can be abruptly changed by charge carriers produced by ionizing radiation in an absorber material. This dependence is sharp even at room temperature, which provides a unique opportunity to deploy graphene in conjunction with narrow-bandgap absorbers (such as InSb) with relaxed temperature, purity, carrier mobility, or lifetime constraints.

Using Monte Carlo simulations (MCNP-Polimi [3]), the interactions of both  $\gamma$ -rays and fast neutrons with various absorber materials (such as Si, Ge, and InSb) were modeled. The energy deposited and location of energy deposition was calculated in configurations resembling our prototype device. For the dominant mode of first interaction (Compton scattering), transport of energetic Compton electrons in the absorber was subsequently modeled using CASINO Monte Carlo code [4]. The calculated ionized charge distribution was used as an input into a COMSOL Multiphysics model [5] to calculate the change in electric field, which results in the modulation of conductivity of the graphene.

We have performed proof-of-concept experiments to study the sensitivity of graphene to a local electric field (using a biased conductive atomic force microscope tip), and the transitory electrical response of a GFET actuated by visible radiation. We have also studied the effect of extensive charged particle irradiation (including ions and electron beams) on GFET, important for the long term robustness and reliability of the graphene based radiation detectors.

## II. PRINCIPLES OF DETECTOR OPERATION

### A. Graphene as a Field-Effect Transistor

Graphene is a monolayer (or few atomic layers) of graphite, which has unique electronic properties [1]. Graphene has a high carrier mobility, about 10 times the mobility of Si at room temperature or better [2]. Graphene also has ultralow electronic noise, and a resistance which is very sensitive to local change of carrier density near the charge neutrality point (CNP) (Fig. 1), or “Dirac point” [6]. This feature has been exploited to detect the adsorption/desorption of a single molecule on graphene [6]. This sensitivity of resistance to charge carriers near the Dirac point allows for graphene to sense small changes in the electric field (Fig. 1) and will be exploited to sense ionizing radiation (that can cause changes in

---

Manuscript received November 13, 2009. This work has been funded by National Science Foundation, Department of Homeland Security, and Department of Defense under awards 0833689-ECCS, 2009-DN-077-AR1036-02, and HDTRA1-09-1-0047 respectively

\*: M. Foxe and G. Lopez made equal contributions to this paper.

<sup>#</sup>: Correspondence should be addressed to I. Jovanovic and Y. P. Chen.

M. Foxe is with the School of Nuclear Engineering, Purdue University, West Lafayette, IN 47907 USA (e-mail: mfoxe@purdue.edu).

G. Lopez is with the School of Electrical Engineering, Purdue University, West Lafayette, IN 47907 USA and with Birck Nanotechnology Center, Purdue University, West Lafayette, IN 47907 USA (e-mail: glopez@ecn.purdue.edu).

I. Childres is with the Department of Physics, Purdue University, West Lafayette, IN 47907 USA and with Birck Nanotechnology Center, Purdue University, West Lafayette, IN 47907 USA (e-mail: almagest@purdue.edu).

R. Jalilian is with the Department of Physics, Purdue University, West Lafayette, IN 47907 USA and with Birck Nanotechnology Center, Purdue University, West Lafayette, IN 47907 USA (e-mail: rjalilia@purdue.edu).

C. Roecker is with the School of Nuclear Engineering, Purdue University, West Lafayette, IN 47907 USA (e-mail: croecker@purdue.edu).

J. Boguski is with the School of Nuclear Engineering, Purdue University, West Lafayette, IN 47907 USA (e-mail: jboguski@purdue.edu).

I. Jovanovic is with the School of Nuclear Engineering, Purdue University, West Lafayette, IN 47907 USA (e-mail: ijovanovic@purdue.edu).

Y.P. Chen is with the Department of Physics, Purdue University, West Lafayette, IN 47907 USA, with the School of Electrical Engineering, Purdue University, West Lafayette, IN 47907 USA and with Birck Nanotechnology Center, Purdue University, West Lafayette, IN 47907 USA (e-mail: yongchen@purdue.edu).

the local electric field). The idea has some analogy with using the sharp feature of the superconductivity transition in a transition edge sensor (TES) [7].

In our prototype device, a GFET has a semiconductor radiation absorber, an oxide dielectric buffer layer, and a layer of graphene on top (Fig. 2). The electric field is created by applying the gate voltage from the back of the absorber to an electrode on the graphene. There are four electrodes on the graphene (for accurate 4-terminal resistance measurement, though 2-terminal measurements would also work as sensors). Two electrodes supply the current through the graphene, and two measure the voltage drop across the graphene, in turn measuring the resistance. The local electric field at graphene affects its resistance via the field effect [2], and the resistance will be most sensitive to the local electric field near the Dirac point (Fig. 1) [6].

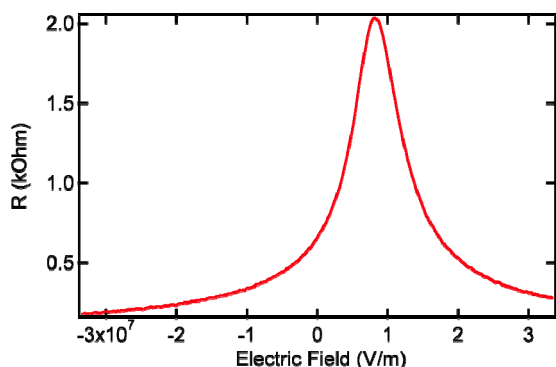


Fig. 1. Graphene exhibits a sharp peak (“Dirac point”) in the resistance as a function of the electric field applied to the graphene sample. Data shown are measured in a representative GFET (Fig. 2, with doped Si as substrate) at room temperature.

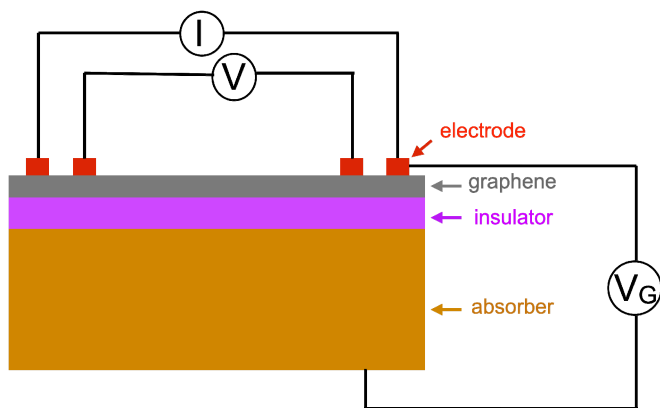


Fig. 2. A GFET consists of an absorber (semiconductor), with an insulator buffer layer which serves as a gate dielectric above.  $V_G$  is the gate voltage applied to the sample. Current is supplied across the graphene sample, and the voltage is measured to calculate the resistance of the graphene layer.

### B. Detection without Drifting the Charges: Ionization-Induced Change of the Electric Field

In a simplest scheme of using a GFET to detect radiation, the electric field at the graphene can be altered by the change

of the resistivity of the absorber upon interaction with ionizing radiation. Using an undoped, insulating (low-conductivity) semiconductor as the absorber, the gate voltage drops across both the absorber and the buffer layer (Fig. 3). With a conductive absorber, the gate voltage drops primarily across the buffer layer, resulting in an increased electric field (Fig. 4).

Radiation interacting with the absorber results in ionization, which can increase the conductivity of the absorber, resulting in an electric field increase (Fig. 4) in the presence of gate voltage applied at the back of the absorber underneath graphene. The change in electric field is indirectly sensed by measuring the resistance of the graphene. This transient change in resistance could be used to detect the presence of radiation interacting with the absorber, and the magnitude of resistance change is related with both the total energy (ionized charges) deposited into the absorber and the location of the ionized charges (Sec. III).

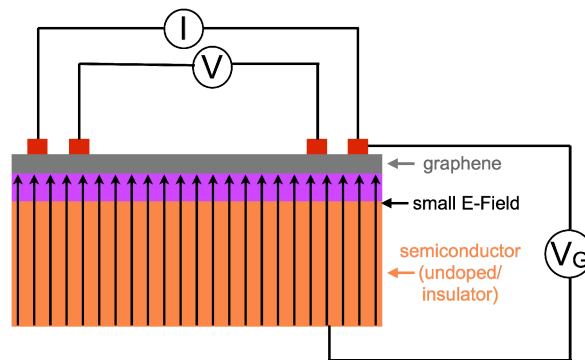


Fig. 3. When the absorber acts as an insulator, the gate voltage drops across both the absorber and the insulator, resulting in a small electric field. With an electric field strength corresponding to the Dirac point, the graphene resistance is at a maximum.

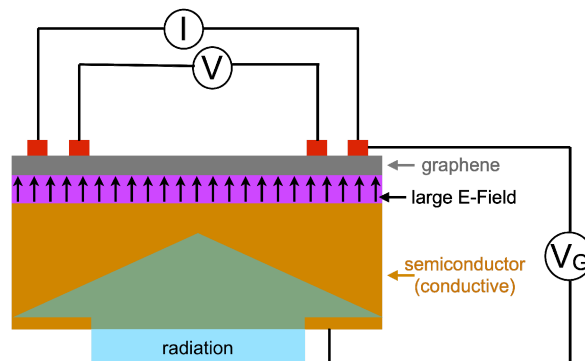


Fig. 4. The incoming radiation ionizes the charges within the (intrinsic) semiconductor to create a conducting absorber. The gate voltage is now effective “transferred” through the absorber and only drops across the insulator. This results in an increased electric field to be detected by the graphene and the resistance changes according to the increased electric field.

### C. Drifting Charges: Detection with Energy Resolution

While the simple scheme described above can detect the presence of ionizing radiation, in many applications such as fissile material detection in nuclear security it is important to measure the energy of the radiation deposited in the absorber. In single-event radiation sensing, the absorber is not ionized

uniformly, and the morphology of charge deposition is highly random (Sec. III). As a result, the electric field change near graphene can have poor correlation with the energy deposited in the substrate, which would compromise the ability to measure deposited energy through change of resistance. This issue can be addressed by drifting the charges to the surface of the absorber, effectively normalizing the position of each interaction to the layer at a constant distance from graphene. A drift electric field can be applied between the back gate electrode (absorber) and the top electrode (graphene). The configuration involving a large back gate electrode and a small graphene creates curved electric field lines, which become denser as they get close to the graphene (Fig. 5 shows a COMSOL [4] simulation). The field lines “funnel” electrons created by the ionizing radiation in the absorber to directly under the graphene, resulting in an electric field response independent of where these ionization occur spatially in the absorber but only dependent on the amount of such ionized electrons (which measures the energy deposited by the radiation).

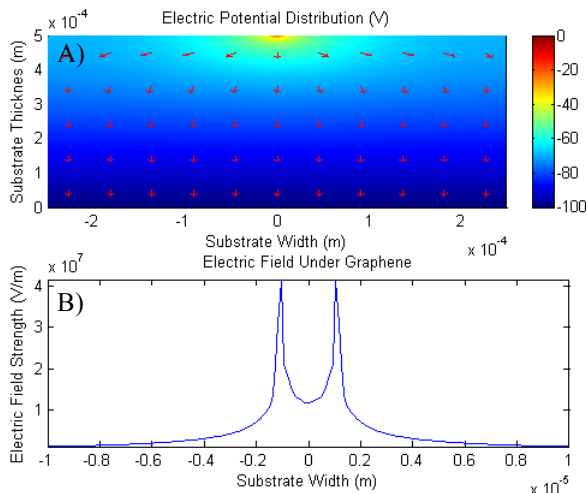


Fig. 5. A) COMSOL simulation of the field lines created with a gate voltage of  $V_G = -100$  V, applied from the electrode on the bottom of the absorber to the graphene (taken to be  $2 \mu\text{m}$  wide in this simulation). The field lines, shown as red arrows, reveal the path of the drifted electrons (note the electron velocity is opposite to the arrow), which converge under the graphene, independent of initial position. B) The line plot shows the electric field strength 5 nm below  $\text{SiO}_2$  near the graphene region.

In a GRD described above, the insulating buffer layer prevents the electrons from flowing out the gate drain electrode. Since the electrons build up under the insulator, the final and maximum change in electric field experienced by the graphene (after all electrons created in one radiation interaction event are drifted under the graphene) is directly related to the number of electrons created. In order to “reset” the sensor, a smaller voltage,  $V_F$ , can be applied horizontally between the doped source and drain, which are embedded in the absorber (Fig. 6). The drift velocity in the transverse direction can be made much smaller than that in the vertical direction, allowing for all of the electrons to settle under the graphene uniformly before they are collected through the

drain. As with a GFET, a constant current flows through graphene during the operation of the detector, and the resistance of the graphene is monitored.

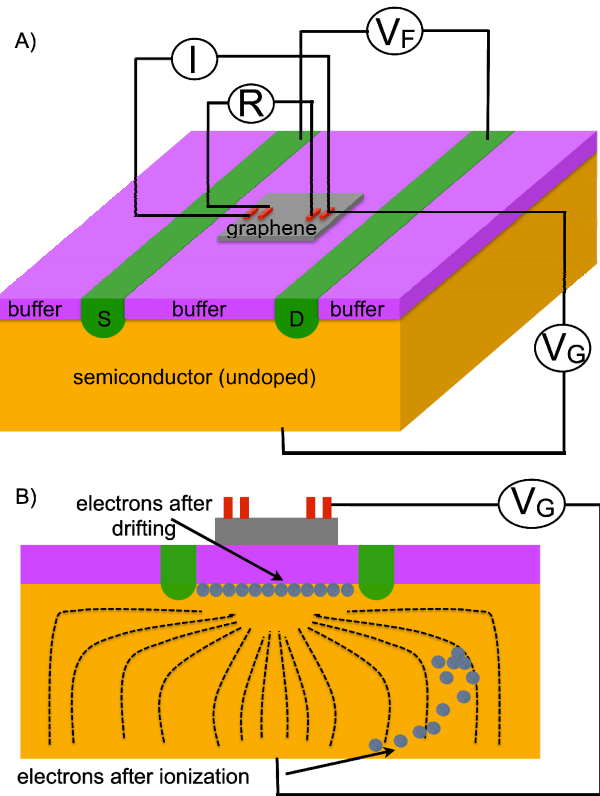


Fig. 6. A) In a GRD, there is an absorber, where the radiation interactions take place. The electrons created by the ionizing radiation are drifted and accumulate between the absorber and the buffer layer. The entire back of the absorber is coated by metal to serve as a gate electrode, while the other electrode is the graphene layer. Applying a gate voltage,  $V_G$ , field lines are produced which direct the electrons towards the graphene. Current is supplied across the graphene sample, and the resistance of the graphene layer is monitored. With the electrons accumulated under the insulator layer, the electric field change measured through the graphene resistance, is directly related to the number of electrons created by the radiation event. A voltage,  $V_F$ , between the source and drain within the absorber slowly drifts the electrons horizontally preventing electron pile-up.  $V_F$  is much smaller than the gate voltage,  $V_G$ , in order to acquire the signal before the electrons drain. B) A cross section of a GRD showing electrons both before and after they are drifted. The path the electrons take is determined from the electric field lines, which are signified by the dotted lines.

### III. DETECTOR MODELING

#### A. Monte Carlo Model for Radiation Interaction

Using MCNP-PoliMi [3], we modeled a Si-based GFET, with a 1 MeV  $\gamma$ -ray source 1 cm from the bottom of the absorber, emitting into  $4\pi$  solid angle. The energy deposited and the position of interaction were calculated in the simulation. From the energies deposited, we modeled the electron trajectories within the silicon using the monte Carlo SIMulation of electroN trajectory in sOLids (CASINO) code [4]. CASINO shows wide variation in electron trajectory, (Fig. 7).

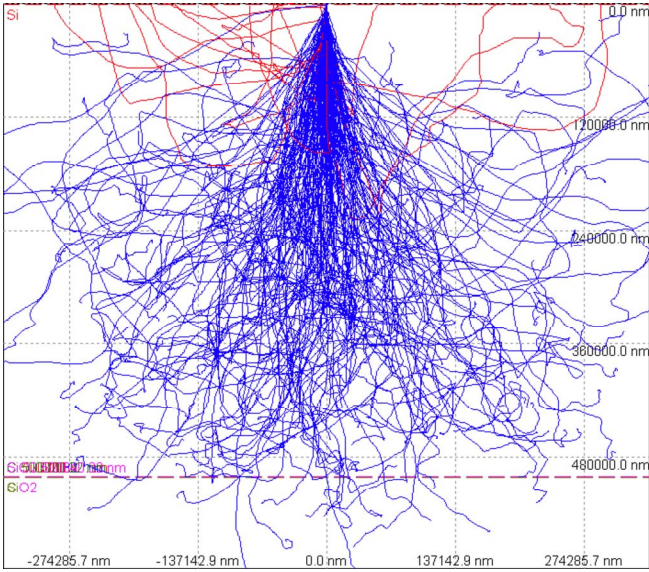


Fig. 7. A CASINO simulation of a beam of 400 keV electrons being emitted normal to a silicon wafer of 500  $\mu\text{m}$ . The red tracks are the electrons which have been backscattered out of the absorber.

As a simple approximation, we treat an electron track as primary and secondary electron regions. The primary region is the start of the electron track and the secondary electron region is the Bragg peak, with a peak to tail ionization ratio calculated from CASINO. The CASINO simulations showed a significant fraction of electrons escaping the Si absorber once they reached energies above  $\sim 400$  keV. For an electron energy of 400 keV, the number of electron-hole pairs created per unit distance within the absorber, (Fig. 8), is calculated using an electron-hole creation energy of 3.66 eV [8].

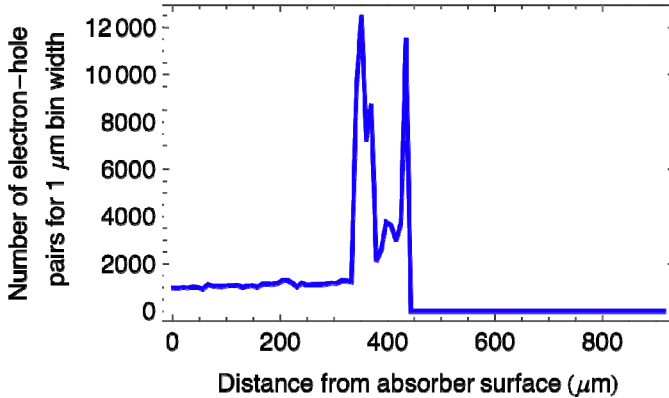


Fig. 8. Shown is number of electron-hole pairs created per 1  $\mu\text{m}$  for a 400 keV electron in a silicon absorber using a 3.66 eV electron-hole creation energy.

### B. COMSOL Model for Electronic Response

In conjunction with the MCNP modeling, finite element method (FEM) simulations were conducted in order to estimate the electric field distribution in a simplified model of the proposed GFET based radiation sensor. The FEM platform utilized in the simulations was COMSOL

Multiphysics 3.5a in the “conductive media DC” application mode for two dimensions. Poisson’s equation was solved in the model:

$$-\nabla \cdot d(\sigma \nabla V - J^e) = dQ_j \quad (1)$$

where  $\sigma$  is conductivity,  $V$  is voltage,  $d$  is the projection into the third dimension,  $J^e$  is external current density, and  $Q_j$  is a current source. For simplicity and without loss of the important physics, the conductivity values for  $\text{SiO}_2$  and the idealized highly insulating intrinsic silicon substrate were taken to be  $1 \times 10^{-14}$  S/m in the model. Since the  $J^e$  and  $Q_j$  parameters were zero in the simulations, Poisson’s equation was reduced to Laplace’s equation.

The simplified device model consisted of a square-shaped highly insulating intrinsic silicon substrate, measuring 500  $\mu\text{m}$  by 500  $\mu\text{m}$ , with a rectangular  $\text{SiO}_2$  top layer, measuring 500  $\mu\text{m}$  by 300 nm. The back gate of the GFET structure was located on the bottom of the Si substrate while the graphene region was modeled as a grounded portion of the top surface of the  $\text{SiO}_2$ . Boundaries at the left and right border of the model were designated as insulating boundary conditions while the interior boundaries were maintained as continuity conditions. A triangular mesh of approximately  $2 \times 10^4$  elements was generated for the simulations.

The simulation investigated the modulation of the electric field due to the generation of charges in the intrinsic silicon substrate following an ionizing event. Carrier concentration data generated by MCNP simulations were used to determine the conductivity of the ionized regions in the model. The conductivities of ionization regions are much larger than the surrounding media (undoped Si or  $\text{SiO}_2$ ). The model assumed that the back gate was biased at 10 V. Fig. 9 illustrates the effect of ionization regions on the distribution of the equipotential lines in the Si absorber for two different energy deposition profiles.

The results from the FEM simulations suggest that, in principle, an ionizing event is able to modulate the electric field in such a way as to produce a substantial change in the resistance of a nearby GFET. In the simulation, the electric field strength in the silicon dioxide immediately above the ionized absorber region was on the order of  $10^6$ - $10^7$  V/m. An electric field as strong as that suggested by the simulation is capable of modulating the number carriers in graphene and produce measurable change of resistance (Fig. 1). Also using COMSOL (FEM) simulation, we have illustrated that a grounded graphene region can serve to “funnel” charge carriers in the ionized absorber towards the Si- $\text{SiO}_2$  interface under a large back gate’s bias (Fig. 5).

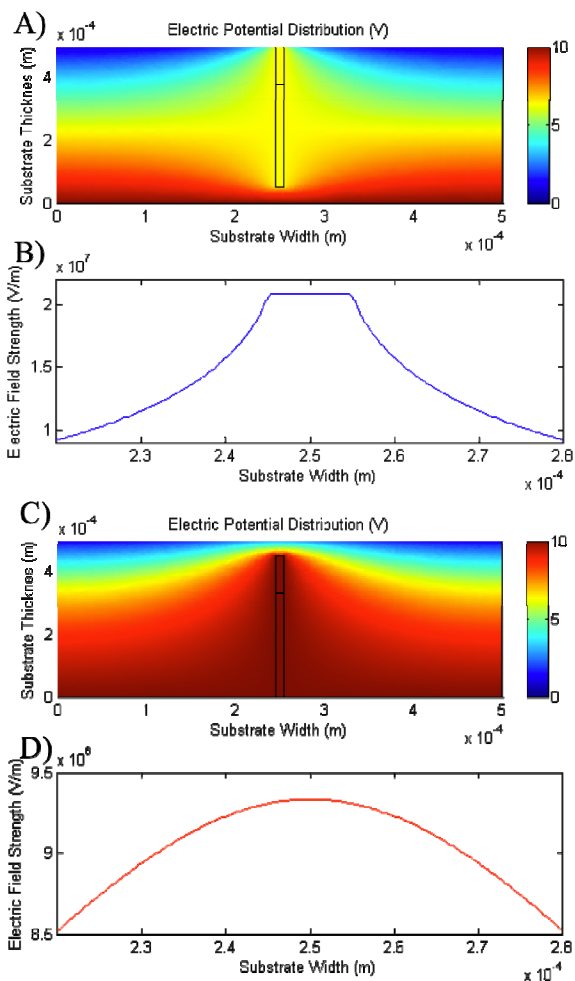


Fig. 9. A) and B) illustrate the distribution of the equipotential lines and electric field 1 nm into the  $\text{SiO}_2$  top surface when the secondary ionization region reaches the  $\text{Si}/\text{SiO}_2$  interface. C) and D) illustrate the distribution of the equipotential lines and electric field 1 nm into the  $\text{SiO}_2$  top surface when the primary ionization region starts from the back gate boundary. The model assumed that the back gate was biased at 10 V. The shape and profile of the ionization region (width=10  $\mu\text{m}$ ) were selected for convenience of simulation and for demonstration purpose. Realistic ionization tracks would have different more complicated profiles.

#### IV. PRELIMINARY EXPERIMENTAL WORK

A series of preliminary experiments were conducted on GFETs in order to better understand the performance metrics of the proposed graphene based radiation sensor. Graphene's sensitivity to localized electric field perturbations was investigated using a novel atomic force microscopy (AFM) top gate probing technique. Proof-of-concept experiments were conducted to study the transient electrical response of GFETs actuated by a photodiode under pulsed HeNe laser irradiation. In addition, the effect of charged particle irradiation on graphene, important for the long term robustness and reliability of the graphene based radiation detector, was investigated. In this preliminary work we used doped Si as the semiconductor substrate in the GFET we fabricated. We are currently

investigating the responses of GFETs with undoped substrates under exposure to gamma rays and X rays of various energies.

##### A. AFM Top Gate: Probing Local Field Response

A schematic of the AFM top gate probing technique used to investigate the sensitivity of graphene to localized electric field perturbations is shown in Fig. 10 A). While in contact mode, a parylene-coated conductive AFM tip was used as a top gate and the resistance of graphene was monitored as the top gate voltage was swept. The graphene device's resistance changed approximately by 120  $\Omega$  with the back gate was grounded when the top gate (AFM tip) voltage was swept from 0 V to 10 V. With the back gate biased to the Dirac point, the resistance of graphene changed approximately by 1 k $\Omega$  for the same range of top gate voltage values. More details of such measurements under various conditions will be presented elsewhere [9]. These results indicate the potential of the graphene-based radiation sensor to sense the localized changes in electric field which could arise from ionization events in the absorber.

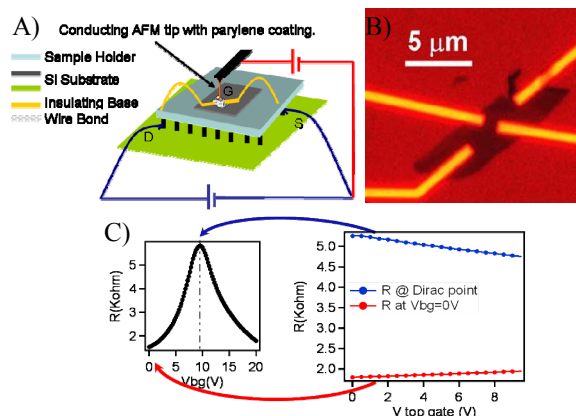


Fig. 10. A) AFM top gate probe schematic. B) Sample GFET. C) Change in resistance due to back gate modulation only (left) and to AFM local top gate sweep (right) for a back gate bias of 10 V (blue) and grounded (red).

##### B. Transient GFET Response under Laser Irradiation

A HeNe laser was used to modulate the back gate voltage of a GFET through a coupled photodiode to illustrate the GFET responses under transient gating (Fig. 11 A), here actuated optically. The drain to source voltage and gate to source voltage was monitored by an oscilloscope to capture the device's response. The frequency of the back gate was controlled by a photodiode incident with a continuous wave laser beam which passed through a programmable signal chopper wheel. Fig. 11 B) shows the photodiode and GFET drain to source voltage, offset for clarity, with the laser beam chopped to 100 Hz. The amplified drain to source signal, gain of 200, demonstrates the prototype sensor's ability to follow the modulated gate signal (also monitored by a photodiode). The observed response of this simple prototype device serves as an operational analog for the transient behavior of the conceived GFET-based radiation sensor when the electric field is modulated (though here externally instead of internally as in our proposed radiation sensor).

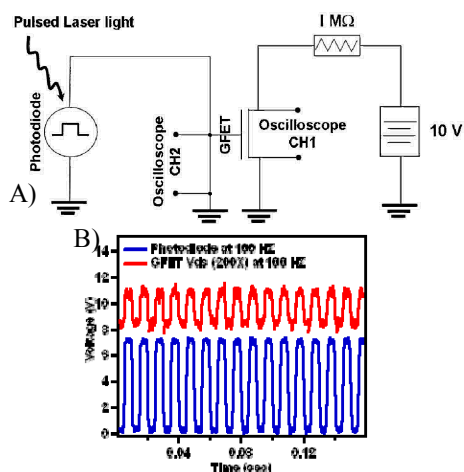


Fig. 11. A) Photodiode and GFET prototype device diagram. B) Photodiode (blue) and GFET (red) response to 100 Hz modulated laser signal.

### C. Electron Beam Irradiation

In order to investigate the GFET's robustness to prolonged exposure to ionizing radiation, three graphene samples were exposed to an electron beam in an EVO 40 SEM system with a 0.15 nA beam current at a 30 keV acceleration voltage over a 50  $\mu\text{m} \times 50 \mu\text{m}$  area for 5 minutes. This gave a dosage of  $112.5 \text{ e}^-/\text{nm}^2$ . These samples typically have a positive CNP because of p-doping caused by environmental impurities such as water. After exposure, the charge-neutral point of all samples shifted to the negative as seen in Fig. 13. In each case, there is also an overall decrease of conductivity, especially at the CNP. The CNP also drifted back toward the original value slowly (days) after the exposure. We interpret these results as a build-up of holes (ionized by the e-beam) trapped at the Si/SiO<sub>2</sub> interface of the substrate. Details of this study are presented elsewhere [10].

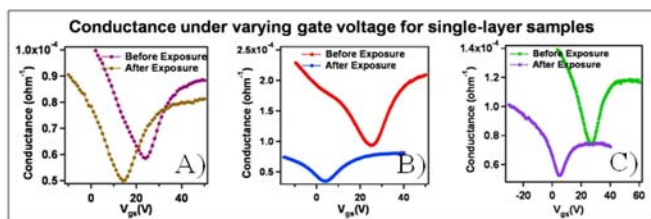


Fig. 12. Gate voltage ( $V_{gs}$ )-dependent conductance measurements made on 3 single-layer graphene samples with a 10 mV drain voltage ( $V_{ds}$ ) for the first sample (A) and 5 mV drain for the others (B,C) both before and after e-beam exposure. Conductance was obtained from the measured 2-terminal current ( $I_{ds}$ ) divided by  $V_{ds}$ .

## V. DISCUSSION AND CONCLUSIONS

Graphene-based sensors have a potential to provide a novel, unique mechanism for detection of ionizing radiation. The sharp transition in resistance as a function of electric field allows the graphene to act as a built-in preamplifier. We can also view the GRD as an (indirect) photoconductor with high gain of transconductance due to the sharp field effect of graphene. We have created a proof of concept model for detecting radiation using a GFET, and performed preliminary proof-of-concept experiments characterizing the response of

GFET to various electrical perturbations. We have also conducted a preliminary design for a graphene-based detector scheme capable of providing energy resolution, and which simultaneously allows for a large scale detector to be operated while using a much smaller size graphene layer. While a conventional MOSFET could also be used for detecting radiations, GFET has a number of potential advantages resulting from the unique properties of graphene, including high speed [11], low noise (even at room temperature) [6] and graphene resistance staying finite [1] in the ambipolar GFET at any carrier densities (while MOSFET channel resistance would diverge when depleted). Various absorber material (including narrow bandgap semiconductors) may be used to optimize the electrical properties and energy resolution in this novel detector.

## ACKNOWLEDGMENT

This research was performed under the project "Graphene-based ultrasensitive advanced radiation detectors" (GUARD), an "Academic Research Initiative" (ARI) program supported by U.S. National Science Foundation Directorate of Engineering and U.S. Department of Homeland Security's Domestic Nuclear Detection Office. YPC also acknowledges the support of the Defense Threat Reduction Agency (DTRA) Young Investigator Program. A portion of M. Foxe's research was performed under the Nuclear Forensics Graduate Fellowship Program which is sponsored by the U.S. Department of Homeland Security's Domestic Nuclear Detection Office and the U.S. Department of Defense's Defense Threat Reduction Agency. We also acknowledge helpful discussions with Prof. Serge Luryi and Dr. Ionel Hau.

## REFERENCES

- [1] A.K. Geim and K.S. Novoselov., "The Rise of Graphene" *Nature Materials*, vol. 6, no. 3, pp. 183-191, March 2007.
- [2] K.S. Novoselov, *et al.* "Electric field effect in atomically thin carbon films". *Science* **306**, pp. 666-669, 2004.
- [3] S. A. Pozzi, E. Padovani, and M. Marseguerra, "MCNP-PoliMi: A Monte Carlo Code for Correlation Measurements," *Nuclear Instruments and Methods in Physics Research Section A*, 513/3 pp. 550-558, 2003.
- [4] P. Hovington *et al.*, *Scanning*, vol. 19, no. 1, pp. 1-14, Jan, 1997
- [5] COMSOL Multiphysics, <http://www.comsol.com>.
- [6] F. Schedin *et al.*, "Detection of individual gas molecules adsorbed on graphene", *Nature Materials*, vol. 6, no. 9, pp. 652-655, Sep.2007.
- [7] S. Friedrich, "Nuclear Diagnostics with Cryogenic Spectrometers," in 11th Symposium on Radiation Measurements and Applications, Ann Arbor, MI, 2006, pp. 157-160.
- [8] N. Tsoulfanidis, "Measurement and Detection of Radiation", 1986.
- [9] R. Jalilian *et al.* in preparation, 2009
- [10] I. Childres *et al.*, Proc. 10th International Conference on Applications of Nuclear Techniques, AIP, 2009
- [11] Y-M. Lin *et al.*, "Operation of Graphene Transistors at Gigahertz Frequencies", *Nano Lett.*, Vol. 9, pp 422-426, 2008
- [12] Y-M. Lin and P. Avouris, "Strong Suppression of Electrical Noise in Bilayer Graphene Nanodevices", *Nano Lett.*, Vol. 8, pp 2119-2125, 2009